Study of the Piezoelectric Power Generation of ZnO Nanowire Arrays Grown by Different Methods

By *Mohammed Riaz, Jinhui Song, Omer Nur, Zhong Lin Wang,* and *Magnus Willander**

The piezoelectric power generation from ZnO nanowire arrays grown on different substrates using different methods is investigated. ZnO nanowires were grown on n-SiC and n-Si substrates using both the high-temperature vapor liquid solid (VLS) and the low-temperature aqueous chemical growth (ACG) methods. A conductive atomic force microscope (AFM) is used in contact mode to deflect the ZnO nanowire arrays. No substrate effect was observed but the growth method, crystal quality, density, length, and diameter (aspect ratio) of the nanowires are found to affect the piezoelectric behavior. During the AFM scanning in contact mode without biasing voltage, the ZnO nanowire arrays grown by the VLS method produced higher and larger output voltage signal of 35 mV compared to those grown by the ACG method, which produce smaller output voltage signal of only 5 mV. The finite element (FE) method was used to investigate the output voltage for different aspect ratio of the ZnO nanowires. From the FE results it was found that the output voltage increases as the aspect ratio increases and starts to decreases above an aspect ratio of 80 for ZnO nanowires.

1. Introduction

Electrical and mechanical coupling phenomena is a feature of some inorganic, organic, and biological systems. The simplest example of linear electromechanical coupling is the piezoelectricity. Among the tetrahedral coordinated wurtzite semiconductors, GaN and ZnO are typical examples.[1] ZnO can be grown in a reproducible way in a variety of nanostructures e.g., nanowires, nanorings, nanobows, platelet circular structures, Y-shape split ribbons and crossed ribbons. This variety can be unique for many applications in nanotechnology.[2] This makes ZnO a technologically important material in many practical applications that requires a large electromechanical coupling. The growth methods[3–5] and electrical and mechanical properties of ZnO nanostructures[6–8] have been extensively studied and by now they are well known to the research community.[9–11] On the other hand, ZnO nanowires have demonstrated sucess in various applications e.g. optoelectronics,[12] biosensors,[13] resonators,[14] electric nanogenerators,[15] and nanolasers.[16] Wang et al. developed a variety of piezoelectric nanogenerators with potential applications for self-powered nanodevices/nanosystems.[17–21] Nevertheless, nanogenerators made of ZnO nanostructures require more research to optimize the electromechanical coupling, thus leading to higher output power.

In this report, a study and comparison of piezoelectric nanogenerators using ZnO nanowires grown on different substrates using low as well as high temperature growth methods is presented. The output potential from each nanogenerator was measured and compared under the same conditions. Finite element method calculation was used to investigate the output voltage signal generated when having ZnO nanowires with different aspect ratios.

2. Results and Discussion

Surface morphology and size distribution of the ZnO nanowires were characterized using LEO 1550 scanning electron microscope (SEM). **Figure 1** shows typical SEM images of the ZnO nanowires grown by both the vapor liquid solid (VLS) and aqueous chemical growth (ACG) methods. Figure 1A,B show SEM images of ZnO nanowires grown on SiC substrate by the VLS method and Figure 1C,D show the case of ZnO nanowires grown on SiC and Si substrates by the ACG method. As can be seen, the nanowires are hexagonally arranged on the substrate. The approximate diameter, length and density of the nanowires were determined to be about 50–100 nm, 3–5 μm, and 3.369×10^7 cm^{-2} on the SiC substrates (Figure 1A) (grown by the VLS method), 200–400 nm, 3–4 μm, and 1.22×10^7 cm^{-2} on the SiC substrates (Figure 1B) (grown by VLS method), 100 nm, 1–2 μm, and 40.50×10^8 cm^{-2} on the SiC substrates (Figure 1C) (grown by ACG method) and 100 nm, 1–2 μm, and 24.0×10^8 cm^{-2} on the Si substrate (Figure 1D) (grown by the ACG method), respectively. It was found that the ZnO nanowires were vertically aligned along the c-axis and distributed uniformly across the entire substrates.

An atomic force microscopy (AFM) Molecular Force Probe MFP-3D from Asylum Research was used to perform the

[*] Dr. M. Riaz, Dr. O. Nur, Prof. M. Willander
Department of Science and Technology
Campus Norrköping
Linköping University
SE-601 74 Norrköping, Sweden
Email: magwi@itn.liu.se
Dr. J. Song, Prof. Z. L. Wang
School of Materials Science and Engineering
Georgia Institute of Technology
Atlanta, GA, 30332–0245, USA

DOI: 10.1002/adfm.201001203

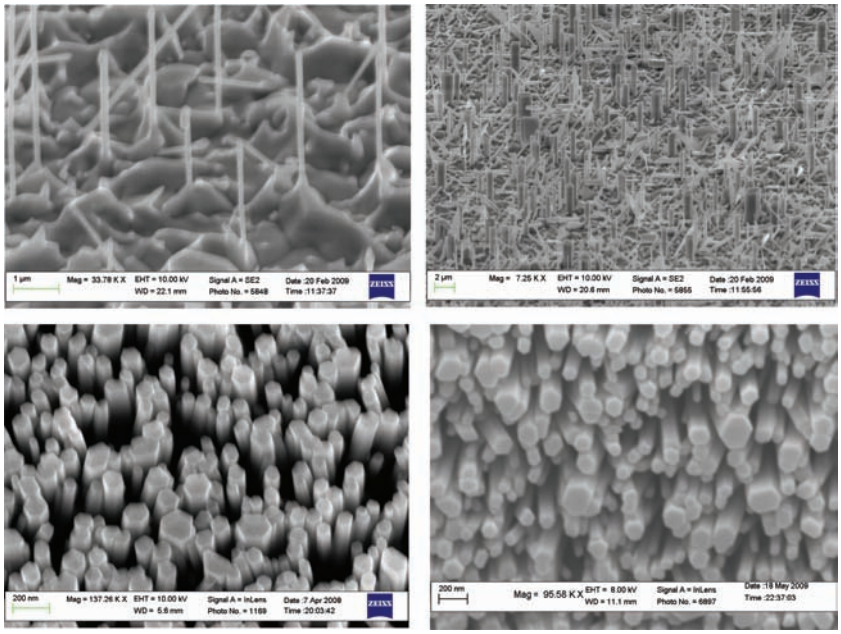

Figure 1. SEM images of aligned ZnO nanowires grown on different substrates. A,B) ZnO nanowires grown on SiC and silicon substrates by the high temperature vapor liquid solid (VLS) method. C,D) ZnO nanowires grown on SiC and Si substrates by the low temperature approach aquoues chemical growth (ACG) method.

experiments with a tetrahedral Si tip (apex angle 70°) coated with Platinum (Pt) film (Electric-Lever AC240 from Olympus), which had a calibrated cantilever normal spring constant of 1.42 N m^{-1}. In contact mode, a constant normal force of 80 nN was maintained between the tip and the sample surface, the scan area was 20 × 20 μm^2. All the measurements were performed at room temperature without biasing the samples. In contact mode, the AFM tip scanned over the top of the ZnO nanowires and the tip height was adjusted according to the top surface of the ZnO nanowire and the local contacting force. In both the VLS and the ACG methods, a thin continuous layer of ZnO (for the VLS case),[15] and a seed layer (for the ACG case)[22] were formed on the substrate. A silver paste was used to make an electric contact at the bottom of the ZnO nanowires. The output signal voltage across an outside a load resistance of R = 500 mega-ohm was continuously monitored as the tip scans over the nanowires. No external voltage was applied during the whole experiment. Both the topography (feed back signal) and the electrical output signals (V) (**Figure 2** and **Figure 3**) across the load were recorded simultaneously. When the AFM tip interacts with the nanowire during scanning, a series of bumps in the topography images were observed reflecting the change in the normal force perpendicular to the substrate. The AFM tip scans line by line at a speed of 30 $\mu m\ s^{-1}$ perpendicular to the vertical direction of the ZnO nanowires.

In Figure 2A,F when the AFM tip interacts transversely with the nanowire, a tensile and a compressive stress and strain are developed on the outer and inner surfaces of the nanowires, respectively. An electric potential distribution is then created by the polarized ions from the tensile to the compressed side surface of the nanowire; this is denoted as V^+ to V^-.[15] The silver electrode at the base of the nanowire was grounded. For a piezoelectric nanogenerator using vertical ZnO nanowires, a Schottky barrier is needed. The I–V behavior of all the samples was tested and measured before performing the piezoelectric scans. Figure 3C,F,I,L show the I–V curves of the different samples, which show a non-linear behavior, revealing that all samples that gave piezoelectric output had a Schottky barrier.

Moreover, in Figure 2 the relation between the output voltage (V) and the topography feed back signals is shown. Wang et al.[15] discussed in details when the AFM tip induced tensile deformation in the ZnO nanowire, a positive potential (V^+) was developed as shown in Figure 3A. When the AFM tip interacted with this potential, the metal tip-ZnO interface becomes reverse biased and a very little current flows across the interface. So no signal was observed as shown in Figure 2B–E. In Figure 2B–E, the feed back signals of the topography have bumps, but still no electrical signals were observed.

On the other hand, when the AFM tip produced a negative strain on the compressed side of the nanowire and interacts with the negative potential (V^-), the metal tip-ZnO will be positively biased and a negative peak of the voltage drop is detected as shown in Figure 2G–J. The negative peak of the output voltage signal is due to the fact that the as-grown ZnO nanowires were n-type semiconductors. Figure 3G–J shows that there is a small offset between the output voltage signal peak and the topography feed back signal peak. The output voltage is seen on the right-hand side of the topography feed back signal with respect to the tip scan direction, which is the compressed side of the nanowire where the metal tip-ZnO interface become forward biased resulting in an electrical output voltage signal.

Figure 3A–F and G–L display the output voltage signal, the 3D images of the density of the output voltage signals recorded during the scanning and the Schottky barrier I–V characteristics of the samples grown by the VLS and the ACG methods. The density of the output voltage signals in the 3D image for the samples grown by the VLS method (Figure 3A–F) is larger than that produced by the samples grown by the ACG method (Figure 3G–J). Also the output voltage signals of the VLS grown samples were higher in magnitude than the ACG grown samples. Two samples of ZnO nanowires were grown on SiC substrate by the VLS method. The same density and magnitude of the average output voltage signals (30–35 mV) was observed from these samples as shown in Figure 3A,B and D,E). Nevertheless, some peaks were as high as 60–90 mV. On the other hand, ZnO nanowires were grown on SiC and Si substrates by the ACG method and these samples had approximately nanowires with the similar morphology and size distribution across the whole substrate. The magnitude of the average output voltage signals from these samples was 5 mV as shown in Figure 3G,H and J,K. Silicon carbide (SiC) was used as a substrate in both growth methods and Si as a substrate in the ACG method only. Almost the same results for one growth

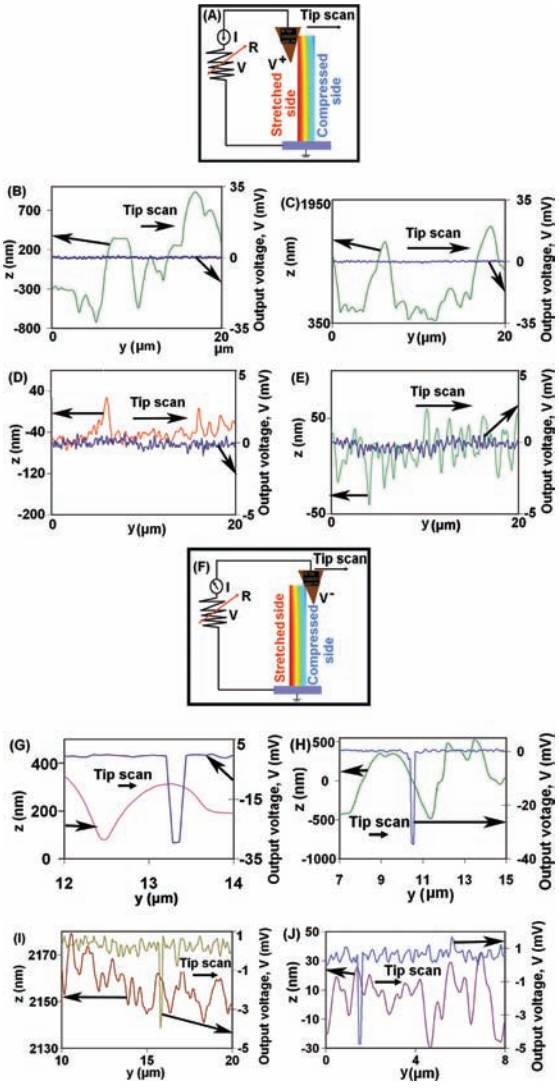

Figure 2. Piezoelectric power generation process by AFM scanning in contact mode over ZnO nanowires array. A,F) Schematic for understanding the electricity output characteristics of the n-ZnO nanowires grown on different substrates. B,C) Samples grown by the VLS method on SiC substrate and D,E) samples grown by the ACG method on SiC and Si substrate shown is the recorded data of the output signal voltage and a typical line scan profile from the AFM feedback topography of the samples. Even though the topography had a bumpy pattern but there is no output voltage signal. This may be due to 1) the AFM tip is interacting with the nanowire on the stretched side resulting of no output signal due to reverse biased Schottky rectifying behavior, 2) the ZnO nanowires may have higher or smaller DOS resulting of no output voltage signal due to the high density of defects and high concentration carriers, 3) the AFM tip may produce a less deformation in the ZnO nanowires due to the higher density, smaller length (in case of ACG grown samples) and larger diameter (in case of VLS grown samples), 4) the AFM tip may have scanned over the gold particle at the top of the nanowire without touching the compressed side of the nanowire in the case of VLS grown samples. Panels (G–J) show the recorded output signal and a typical line scanning profile from the AFM feedback topography of the samples. G,H) For the samples grown by VLS method on SiC substrate and I,J) for the samples grown by the ACG method on SiC and Si substrates, respectively. The output signals voltage is exactly emerging when the AFM tip passed over the compressed bent side of the nanowire.

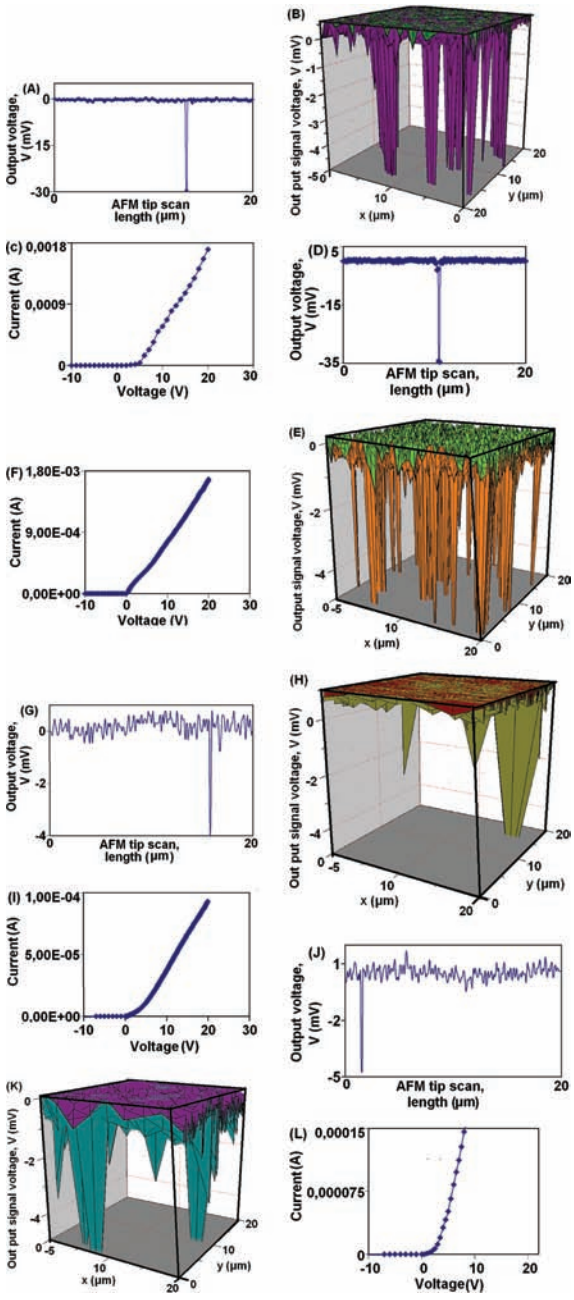

Figure 3. Comparative performance of the ZnO nanogenerators grown by the VLS and ACG methods on SiC and Si substrates, respectively. Panels (A–C) and (D–F) show the output signal voltage, 3D plot of the density of output signals, and the *I–V* measurements for samples grown on SiC substrate by the VLS method. Similarly (G–I) and (J–L) show the output signal voltage, 3D plot of the density of output signals, and the *I–V* measurements for the samples grown on SiC and Si substrates by the ACG method. The nano-generators from ZnO nanowires grown by VLS method have higher output signals density (B,E) and larger magnitude of the output signals (A,D) compared to nano-generators from ZnO nanowires grown by the ACG method (H,K) and (G,J). The magnitude and density of the output signals generated from the samples grown by the VLS method on SiC substrates are almost the same and similar for the samples grown by the ACG methods on SiC and Si substrates having the same magnitude and density of the output signals. This observation significantly reveal that the performance of the ZnO nanogenerator does not depend on the substrates and mainly depends on the growth method and quality of the nanowires.

method and the same results for the other growth method were obtained. These observations revealed that the substrates has no effect on the performance when considering the output voltage signal. This was due to the fact that our nanogenerators were working on the principle of direct current (DC) as opposed to the surface acoustic wave (SAW) devices, where the performance of the devices were strongly dependent on the piezoelectric ZnO under layer substrate.[29]

The differences in the output voltage signals of the samples grown by the VLS and the ACG methods may be due to four different reasons:

1) Density of states (DOS): DOS depends mainly on the doping concentration. Materials with high doping concentration yield higher DOS and hence higher conductivity. If the Schottky barrier formed at the metal Pt-ZnO interface was sufficiently low (due to high DOS and high carrier conductivity), the electrons could effectively tunnel through the barrier resulting in a linear *I–V* behavior i.e., ohmic, which is severely affects the conduction and output signals. Similarly, a lower DOS also affects the output signal of the nanogenerator due to the fact that a lower charge carrier concentration requires a higher potential difference in the device for the output signal and the conduction of the carries in the outer circuit. In both situations, no output signal was observed (Figure 2B–E).

On the other hand for medium doped ZnO nanowires, the depletion region extended far into the semiconducting material and a reasonable voltage is necessary for the relaxation of the dipole charges developed (due to direct piezoelectric effect) across the unit volume of the ZnO nanowire. In this case a non-linear *I–V* behavior will be developed between the metal tip and ZnO nanowire surface, leading to carrier's conduction and output signals across the load circuit as shown in Figure 2F–J. ZnO nanowires grown by the ACG method have higher density of state compared to the nanowires grown by the VLS method due to the higher intrinsic doping concentration. Thus nanogenerators based on the ACG grown samples are expected to yield smaller output voltage signals compared to those grown by the VLS method.

2) Surface morphology: surface morphology, such as surface roughness, might had influenced the electrical transport properties of the ZnO nanowires. In some cases, crystalline imperfections in the outermost layer were observed. Lin et al.[24] found that, even if the nanowires were grown under identical conditions, some nanowires were covered with a non-crystalline or amorphous layer, while others showed perfect crystalline structure even at the boundary layer. The origin of the amorphous layer was not then clear. Comini et al.[25] has observed this thin amorphous layer from transmission electron microscope images and suggested that this may be due to the formation of condensate of the vaporized material during cooling in the growth process.

3) Structural differences due to the growth temperature: the high temperature and low temperature approach, affected the crystal quality as well as the defect density in the nanowires. Density of defects in the crystal and at the metal ZnO surface interface can also affect the output signal. Brillson et al.[23] showed that low-defect crystals of ZnO exhibited strongly rectifying *I–V* characteristic while high-defect density crystals showed ohmic behavior. Their results showed that resident native defects in ZnO single crystals and native defects created by the metallization process dominate metal-ZnO Schottky barrier behavior and affects the ideality factor. They also showed that the reverse current was less for low defect crystal compared to high defect crystal. They also suggested that the reverse current increases with increasing defect density.

The precursor or the catalyst might have an influence on the number of defects (like incorporated impurity atoms) in the nanowires. Schlenker et al.[26] compared the resistivity of nanowires grown in a catalyst-assisted process with those grown without the use of a catalyst. They observed that the catalyst assisted grown nanowires exhibited a smaller resistance than those grown without catalyst. In this regard the samples grown by the VLS method were with gold catalyst assisted and exhibited a smaller resistance than samples grown by the ACG methods.

4) Aspect ratio and density of the nanowires: The aspect ratio and density of the ZnO nanowires across the substrates can also influence the output signals. Wang et al.[15] showed that a maximizing the deflection of the nanowire yielded higher output voltage signals. In our case, the samples grown by the VLS method were less dense than those grown by the ACG method. The effect of the density was that the deflection of the nanowires by the AFM tip during scanning was less and thus yielded either no or smaller magnitude of the output signal (Figure 2B–E, I,J) as compared to the less dense samples (Figure 2G,H). The aspect ratio also affected the output voltage signal of the nanogenerator. The finite element (FE) calculation method was used to investigate the effect of the length and diameter (aspect ratio) on the output electrical potential of ZnO nanowires based nanogenerator. The FE program solves the following equations[28]:

$$\sigma_{\mathrm{p}} = c_{\mathrm{pq}}\varepsilon_{\mathrm{q}} - e_{\mathrm{kp}}E_{\mathrm{k}} \quad (1)$$

$$D_{\mathrm{i}} = e_{\mathrm{iq}}\varepsilon_{\mathrm{q}} + k_{\mathrm{ik}}E_{\mathrm{k}} \quad (2)$$

Where σ is the stress tensor, c_{pq} is the linear elastic constant, ε_{q} the strain tensor, e_{iq} is the piezoelectric coefficient, k_{ik} is the dielectric coefficient, D is the electric displacement´, and E is the electric field. The elastic, dielectric and piezoelectric coefficients constants values of ZnO from the materials library of Cosmol mulit-physics program were used.[27]

Figure 4 is a typical FE simulation result and the schematic shows how the lateral force is applied to bend the nanowire. A nanowire of 1000 nm length with a diameter of 50 nm was used for the simulation shown in Figure 4. Similarly the electrical potential from nanowires at constant diameter of 50 nm with changing the length from 600 nm to 6000 nm was investigated (**Figure 5**). From Figure 5 it was observed that the calculated output electrical potential was increasing for lengths of 600 to 4000 nm and then it decreases upon any further increase of the length. As the length is increased the aspect ratio also increases and the deflection of the nanowire increases. This leads to an increase in the output electrical potentials up to an aspect ratio of 80 (at a length of 4000 nm and a fixed diameter of 50 nm). Upon further increase in the length (increase of the aspect ratio) the output voltage signal starts to decrease. The decrease in the output electrical potential was due to the excessive deflection in

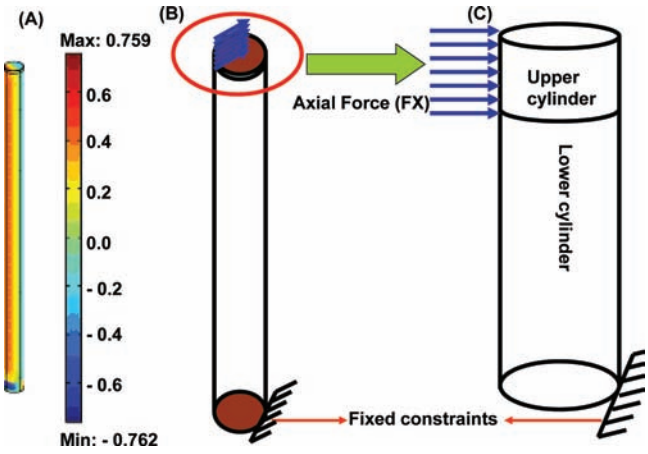

Figure 4. A typical FE result of a ZnO nanowire having an aspect ratio of 20. A) A none distorted ZnO nanowire after FE simulation. B) Schematic model with a force applied at the top edge of the ZnO nanowire. C) The enlarged view of the top portion when the force is applied in the FE simulations.

the nanowire in both the lateral and the vertical directions. This excessive deflection in the nanowire might cause a screening of the charge carriers on the outer surfaces of the nanowires resulting in a decrease of the electrical potential.

Figure 6 shows the electrical potential versus the aspect ratio of different nanowires of a length of 1000 nm and a diameters between 8–83 nm. From Figure 6 it is shown that the output electrical potential is increasing with decreasing the diameter of the nanowires and become less effective below a diameter of 12.5 nm. As the diameter is decreasing the aspect ratio is increasing and the deflection of the nanowire increases yielding an increase in the output electrical potentials up to a diameter of 12.5 nm. With further increase in the aspect ratio no effect on the output voltage signal was observed. During all these calculations the lateral force was kept constant i.e., 80 nN.

From Figure 5 and 6, it was also observed that the magnitude of the output voltage signal is different for the same aspect ratio. In Figure 6 the magnitude of the output voltage signal is higher than in Figure 5. This is due to the geometry used to apply the

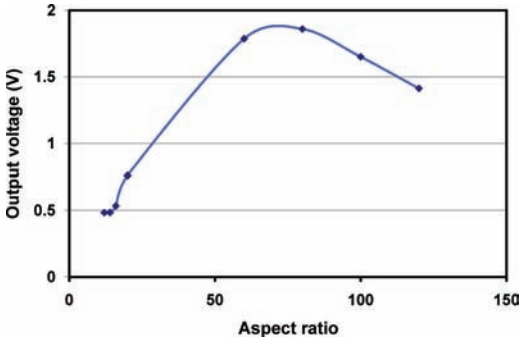

Figure 5. Output electrical potential vs aspect ratio of ZnO nanowires controlled at constant diameter of 50 nm and changing the nanowire length from 600 nm to 6000 nm.

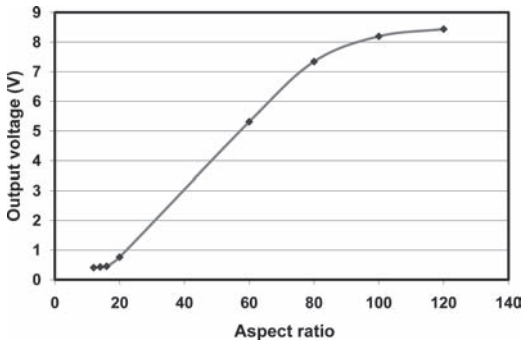

Figure 6. Output electrical potential vs aspect ratio of ZnO nanowires controlled at constant length of 1000 nm and changing the nanowire diameter from 8 nm to 83 nm.

force for bending the nanowire. In our experiment, the ZnO nanowires were bent by an AFM tip during scanning at constant force of 80 nN. The AFM tip has a finite size and thus the force was applied per unit area on the side of ZnO nanowire. In simulation the continuum geometry is divided into discrete regions and the solution is always obtained on only a limited number of discrete points on the mesh. The result of the simulation depends on the mesh size. The simplest method is to use a point force but this is not realistic due to the divergence of the solution. The exact contact area of the AFM tip with the surface of the ZnO nanowires is not known. To simulate with conditions as close as possible to the experiment, the nanowire was modeled as consisting of two cylinders placed one on top of each other. The size of the top cylinder was selected for each aspect ratio in the simulation to maintain a constant force of 80 nN m^{-2}. The force was applied to the smaller cylinder at the top as shown in Figure 4C. In case of the variation of aspect ratio by changing the diameter (Figure 6), the size of the top cylinder was selected such that a constant force is maintained. These results also suggest that to obtain a maximum voltage the contact area must be maximized along the length of the nanowire instead of maximization along the diameter of the nanowire.

From these calculations it was concluded that for different ZnO nanowires with the same aspect ratios (different lengths and diameters) different results are achieved regarding the electrical potentials when the same lateral force is used.

3. Conclusion

The performance of piezoelectric power nanogenerators fabricated using ZnO nanowires grown by high and low temperature approaches (VLS and ACG) on n-SiC and n-Si substrates is presented and analyzed. The VLS grown samples have yielded an average of 30–35 mV while the ACG grown samples yielded an average of 5 mV output voltage signals. It was observed that the performance of the nanogenerators was not dependent on the substrates but mainly depends on the crystal quality, effective length, diameter and density of the nanowires across the substrates. The VLS grown samples were more suitable for efficient operation of the piezoelectric power nanogeneration compared

to the ACG grown samples. Finite element simulation was used and it was found that the output voltage of the nanogenerator increased as the aspect ratio is increased until a value of 80. For ZnO nanowires having an aspect ratio higher than 80, the out put voltage was found to be decreasing. Also from the FE results it was found that the output voltage from ZnO nanowire could be maximized by increasing the contact area along the length of the nanowire. From our experiments and FE calculations it was concluded that to achieve a higher density and larger magnitude of the output voltage signals from a ZnO nanogenerator, the density of the nanowires on the substrate, length, and diameter of the nanowires should all be in the range of 10^6 to 10^7 cm^{-2}, 1 μm to 4 μm, and 50 nm to 200 nm, respectively.

4. Experimental Section

The ZnO nanowires/nanorods used in the present experiments were grown on SiC and Si substrates by the ACG and the VLS methods. In the ACG method, zinc nitride-dihydrate [$Zn(NO_3)_2{\cdot}6H_2O$] was mixed with hexamethylenetetramine (HMT) ($C_6H_{12}N_4$) by the same molar concentration for both solutions. The molar concentration was varied from 0.025 to 0.075 M. The two solutions were stirred together and the substrates were placed inside the solution. Then, the solution was heated up to 90 °C and kept at that temperature for 3 h. Before the substrates were placed inside the solution, they were coated with a ZnO seed layer using the technique developed by Greene et al.[22] Zinc acetate dihydrate was diluted in ethanol to a concentration of 5 mM. Droplets of the solution were placed on the substrate until they completely covered the surface. After 10 s, the substrates were rinsed in ethanol and then dried in air. This procedure was repeated five times and then the samples were heated to 250 °C in air for 20 min to yield a seed layer of ZnO particles on the substrates. The whole procedure was repeated twice in order to ensure a uniform ZnO seed layer. The side of the substrate with the seed layer was mounted face down in the solution. After the growth, the samples were cleaned in de-ionized water and left to dry in air inside a closed beaker.

In the VLS technique, ZnO powder (99.9%) was mixed with graphite powder in a weight ratio of 1:1. Typically, 50–70 mg of the mixed powder was placed in a ceramic boat and the boat was then placed inside a quartz glass tube. The substrates were coated with a thin metal layer functioning as a catalyst and placed on top of the powder. In this study, gold (Au) with a thickness of 1–5 nm was used as a metal catalyst. The side of the substrate coated with Au was placed face down, toward the powder. The distance between the powder and the substrate was about 3 mm. The growth temperature was varied between 890 and 910 °C and the growth time was varied between 30 and 90 min.

Acknowledgements

M.W. thanks the Swedish Research Council for financial support.

Received: June 13, 2010
Published online:

[1] A. D. Corso, M. Posternak, R. Resta, A. Baldereschi, *Phys. Rev. B* **1994,** *50*, 10715.
[2] Z. L. Wang, *Mater. Sci. Eng. R* **2009**, *64*, 33.
[3] M. Aoki, K. Tada, T. Murai, *Thin Solid Films* **1981**, *83*, 283.
[4] X. W. Sun, H. S. Kwok, *J. Appl. Phys.* **1999**, *86*, 408.
[5] H. B. Kang, K. Nakamura, S. H. Lim, D. Shindo, *J. Appl. Phys.* **1998**, *37*, 371.
[6] M. Riaz, O. Nur, M. Willander, P. Klason, *Appl. Phys. Lett.* **2008**, 92, 103118; b) M. Riaz, O. Nur, M. Willander, P. Klason, *Appl. Phys. Lett.* **2008**, *92*, 179902(E).
[7] M. Riaz, A. Fulati, Q. X. Zhao, O. Nur, P. Klason, M. Willander, *Nanotechnology* **2008**, *19*, 415708.
[8] M. Riaz, A. Fulati, L. L. Yang, O. Nur, M. Willander, P. Klason, *J. Appl. Phys.* **2008**, **104**, 104306.
[9] J. D. Albrecht, P. P. Ruden, S. Limpijumnong, W. R. L. Lambrecht, K. F. Brennan, *J. Appl. Phys.* **1999**, *86*, 6864.
[10] E. M. C. Fortunato, P. M. C. Barquinha, A. C. M. B. G. Pimentel, A. M. F. Goncalves, A. J. S. Marques, R. F. P. Martins, L. M. N. Pereira, *Appl. Phys. Lett.* **2004**, *85*, 2541.
[11] R. L. Hoffman, *J. Appl. Phys.* **2004**, *95*, 5813.
[12] M. Willander, O. Nur, Q. X. Zhao, L. L. Yang, M. Lorenz, B. Q. Cao, J. Z. Pérez, C. Czekalla, G. Zimmermann, M. Grundmann, A. Bakin, A. Behrends, M. Al-Suleiman, A. El-Shaer, A. C. Mofor, B. Postels, A. Waag, N. Boukos, A. Travlos, H. S. Kwack, J. Guinard, D. L. S. Dang, *Nanotechnology* **2009**, *20*, 332001.
[13] S. Al-Hilli, A. Öst, P. Strålfors, M. Willander, *J. Appl. Phys.* **2007**, *102*, 084304.
[14] X. D. Bai, P. X. Gao, Z. L. Wang, E. G. Wang, *Appl. Phys. Lett.* **2003**, *82*, 4806.
[15] Z. L. Wang, J. H. Song, *Science* **2006**, *312*, 242.
[16] Q. X. Zhao, P. Klason, M. Willander, P. J. Bergman, W. L. Jiang, J. H. Yang, *Phys. Scr.* **2006**, *T126*, 131; H. Zhou, M. Wissinger, J. Fallert, R. Hauschild, F. Stelzl, C. Klingshirn, H. Kalt, *Appl. Phys. Lett.* **2007**, *91*, 181112.
[17] R. Yang, Y. Qin, C. Li, G. Zhu, Z. L. Wang, *Nano Lett.* **2009**, *9*, 1201.
[18] X. D. Wang, J. H. Song, J. Liu, Z. L. Wang, *Science* **2007**, *316*, 102.
[19] M-Pei. Lu, J. Song, M-Yen. Lu, M-Teng. Chen, Y. Gao, L-Juann. Chen, Z. L. Wang, *Nano Lett.* **2009**, *9*, 1223.
[20] R. S. Yang, Y. Qin, L. Dai and Z. L. Wang, *Nat. Nanotechnol.* **2009**, *4*, 34.
[21] Y. Qin, X. D. Wang, Z. L. Wang, *Nature* **2008**, *451*, 809.
[22] L. E. Greene, M. Law, D. H. Tan, M. Montano, J. Goldberger, G. Somorjai, P. D. Yang, *Nano Lett.* **2005**, *5*, 1231.
[23] L. J. Brillson, H. L. Mosbacker, M. J. Hetzer, Y. Strzhemechny, G. H. Jessen, D. C. Look, G. Cantwell, J. Zhang, J. J. Song, *Appl. Phys. Lett.* **2007**, *90*, 102116.
[24] Y.-F. Lin, W.-B. Jian, C. P. Wang, Y.-W. Suen, Z.-Y. Wu, F.-R. Chen, J.-J. Kai, J.-J. Lin, *Appl. Phys. Lett.* **2007**, *90*, 223117.
[25] E. Comini, G. Faglia, M. Ferroni, G. Sberveglieri, *Appl. Phys. A* **2007**, *88*, 45.
[26] E. Schlenker, A. Bakin, T. Weimann, P. Hinze, D. H. Weber, A. Gölzhäuser, H.-H. Wehmann, A. Waag, *Nanotechnology* **2008**, *19*, 365707.
[27] COMSOL MULTIPHYSIC, version 3.5.
[28] M. A. Schubert, S. Senz, M. Alexe, D. Hesse, U. Gösele, *Appl. Phys. Lett.* **2008**, *92*, 122904.
[29] C. Jagadish, S. J. Pearton, *Zinc Oxide Bulk, Thin Films and Nanostructures*, 1st Edition, Elsevier, UK **2006**.